Electric Power Systems Research 171 (2019) 150–157

Contents lists available at ScienceDirect

Electric Power Systems Research

journal homepage: www.elsevier.com/locate/epsr

Resilient design of large-scale distribution feeders with networked microgrids

Arthur Barnes*, Harsha Nagarajan, Emre Yamangil, Russell Bent, Scott Backhaus

Los Alamos National Laboratory, PO Box 1663, Los Alamos, NM 87545, USA

ARTICLE INFO

Keywords:
Resilience
Electric distribution
Mixed integer linear optimization

ABSTRACT

Electrical distribution systems are often vulnerable to severe weather. Upgrades, such as microgrids, system hardening, and line redundancy, can greatly reduce the number of electrical outages during such extreme events. More recently, the networking of microgrids has received attention as a solution to further improve the resilience of distribution feeders. Although these upgrades have the potential to improve resilience, a barrier to their execution is a lack of tools and approaches that support systematic exploration of the underlying parameters of these upgrades and their cost vs. resilience tradeoffs.To address this gap, we develop a method for designing resilient distribution grids, including networked microgrids, by posing the problem as a two-stage stochastic program. When resilience is defined as the ability of a network to supply load immediately following a storm event, we show that a decomposition-based heuristic algorithm scales to a 1200-node distribution system. We also vary the study parameters, i.e., the cost of microgrids relative to system hardening and target resilience metrics. In this study, we find regions in this parametric space that correspond to different resilient distribution system architectures, such as individual microgrids, hardened networks, and a *transition region that suggests the benefits of microgrids networked via hardened circuit segments*.

1. Introduction

Recent extreme weather events, such as Hurricane Sandy in 2012 and Hurricanes Harvey, Irma, and Maria in 2017, demonstrated shortcomings in the resilience of the North American power grid. Under a definition of resilience that measures the ability to operate a grid during and immediately after severe events such as earthquakes, ice storms, hurricanes, and wildfires [1], transmission grids are generally considered resilient because of meshed lines and generation reserves. In contrast, distribution grids are much less resilient under these conditions; some studies estimate that as many as 80% of all outages originate at the distribution level [2]. Factors contributing to this lack of resilience include radial configurations, higher component damage susceptibility, and limited controllable generation [3].

Based on these observations, and the prolonged outages caused by Hurricane Sandy, the US Department of Energy (DOE) identified distribution grid resilience under severe weather as a research area with significant gaps, including a lack of design tools that include resilience metrics [4]. Specifically, microgrids, collections of generation and loads that can be disconnected during severe events to operate as standalone grids [5], were identified as technologies for improving resilience. More recent work has suggested that networking microgrids can further enhance the resilience benefits of microgrids [6]. However, it is important to note that other options are available to improve resilience, e.g., improved vegetation management, physical reinforcement of overhead structures, and the addition of new lines and switching to increase circuit redundancy [1,3,5]. Although this and other work on distribution system resilience has demonstrated the value of these improvements, how to *model all these improvements simultaneously and tractably find actionable solutions on large-scale systems* remains an open question.

To address these gaps, this manuscript develops a resilient design method to upgrade distribution networks to meet resilience targets during severe events. The objective of the design method is to upgrade a distribution network to meet near-term resilience requirements, defined in terms of fraction of load met. However, it is possible it extend the method to produce a solution that is economic over a planning horizon, or to add a cost term to account for load interruption costs in addition to load served requirements. The method combines five challenging features of resilience modeling in power systems: resiliency metrics, system operations, power flow physics, system design, and solution validation.[1] The

* Corresponding author.
E-mail address: abarnes@lanl.gov (A. Barnes).

[1] Our preliminary work on this topic appears as a conference paper in [7]. This paper neglected power flow physics and solution validity. It was also restricted to small-scale synthetic test systems.

https://doi.org/10.1016/j.epsr.2019.02.012
Received 10 March 2018; Received in revised form 29 January 2019; Accepted 11 February 2019
Available online 26 February 2019
0378-7796/ Published by Elsevier B.V.

resiliency metrics are based on a stochastic programming model [7–9] that requires the distribution network to meet resilience requirements over scenarios of widespread network damage from severe weather. Such models are difficult to solve when the number of scenarios is large. To address this challenge, we developed a decomposition-based approach that leverages the natural separable structure of the scenarios.

System operations and constraints include those that are commonly used in distribution circuits, i.e., line and voltage limits. Most of these constraints are straightforward to model, except for requirements that distribution networks operate in a radial fashion. In the worst case, enforcing this constraint requires enumerating all possible cycles (loops) in the network and formulating constraints that eliminate them—an NP-complete problem [10]. To address this computational challenge, some existing work has formulated this constraint with flow-based formulations [11]. Although the number of constraints in this formulation is polynomial, formulations with these constraints are generally hard to solve because the linear programming relaxation is weak. Instead, we use a cut-based approach. In the worst case, the cut-based formulation requires an exponential number of constraints. However, it has a better polyhedral structure, making it easier to solve [12].

The *power flow physics* are based on the nonconvex, unbalanced multiphase AC power flows of distribution networks and are combined with discrete *system design* options. Within the literature, a number of relaxations and linear approximations have been developed for radial networks to make these equations tractable [13–17]. However, the current state of the art in nonconvex solvers restricts the direct application of such models to networks of small size. Thus, we use the linear approximation presented in [14,15] and generalize it to handle design (on/off) constraints with a disjunction formulation.

Finally, although the resulting formulation is generally more tractable, it is possible that the solutions based on this formulation are physically infeasible. To address this challenge, we develop a method that *verifies and validates* the quality of the solutions using OpenDSS [18], a distribution system simulator. This takes into account the nonlinear voltage drop along lines with respect to power flow and the effect of line charging capacitance.

Literature Review Recently, [19] addressed the problem of placing microgrids for optimal restoration by topology reconfiguration using a Viterbi algorithm. Their approach is a heuristic-based method that is limited to balanced systems of small scale (up to 69 buses). In [20], a method was developed to design resilient distribution systems by multiple microgrid formations (up to 615 buses). Their work focused on topology reconfiguration of grids and uses balanced Lin-Dist to model power flow physics. Their model is focused on operating existing networks rather than considering new designs. Radial topologies are enforced using flow constraints (we use the cut-based formulation). Related approaches, such as [21,3], use a defender-attacker-defender (DAD) model that finds a small set of critical upgrades that enable resilience to targeted attacks. In principle, the DAD approach can be used for widespread extreme weather event damage, but in practice, the computational complexity of a DAD approach grows quickly with the number of allowable failed components because of its bilevel structure. Thus, DAD approaches are often intractable for our network design problem.

Other recent noteworthy studies address microgrid operation but not the placement of components such as generation and switches. These include [22], which applies a mixed-integer linear approach to coordinate automatic switches and distributed generation to maximize the amount of critical load restored. A similar approach is described in [8], which accounts for stochastic renewable generation when determining switch settings to restore load after a disaster event. In [23], the authors investigate coordination of multiple networked microgrids on a distribution feeder. Lastly, [24] presents a communication architecture for coordination of networked microgrids and demonstrates the feasibility of the architecture via a hardware-in-the-loop testbed.

In the context of the existing literature, the key contributions of this paper include the following:

- A model of resilient distribution system design that simultaneously considers hardening options, redundancy options, microgrids, and networked microgrids
- An algorithm for finding resilient distribution system designs that scales to distribution circuits with up to 1200 nodes
- The introduction of full unbalanced power flows to validate the physical viability of the resilient system design solutions
- A system study on a real distribution circuit that shows the parametric space where different design options are the most cost-effective for achieving resilience

The rest of this manuscript is organized as follows. Section 2 describes the nomenclature of the resiliency model. Section 3 describes the formulation and algorithm. Section 4 discusses the numerical experiments. Section 5 presents results of those experiments, and Section 6 concludes the paper.

2. Nomenclature

Complex quantities (variables and constants) are denoted in bold. Given any two complex numbers $\boldsymbol{z}_1$ and $\boldsymbol{z}_2$, $\boldsymbol{z}_1 \geq \boldsymbol{z}_2$ implies $\Re(\boldsymbol{z}_1) \geq \Re(\boldsymbol{z}_2)$ and $\Im(\boldsymbol{z}_1) \geq \Im(\boldsymbol{z}_2)$.Parameters$\mathcal{N}$set of nodes (buses).$\mathcal{E}$set of edges (lines and transformers).$\mathcal{P}_i$set of phases allowed to consume or inject power at bus i.$\mathcal{P}_{ij}$set of phases for line (i, j).$\mathcal{L}$set of all loads.$\mathcal{K}$set of all critical loads.$\mathcal{G}$set of existing and candidate microgrids.$\mathcal{S}$set of disaster scenarios.set of edges that are inoperable during $s \in S$.$\mathcal{C}$set of sets of nodes that include a cycle.$\bar{\boldsymbol{S}}^d_{l,k}$complex power demand in kVA for load on phase k of load l.$\bar{\boldsymbol{S}}^d_{l,k}$complex power demand in kVA for load on phase k of load l.$\bar{S}^k_{ij}$line capacity in kVA between bus i and bus j on phase k.λfraction of critical load power that must be served.γfraction of total load power that must be served.$\bar{\boldsymbol{S}}^g_{l,k}$generation capacity in kVA on phase k of distributed generator l.β_{ij}parameter for controlling how much variation in flow between the phases is allowed on line (i, j).$\boldsymbol{S}^{k,s,l}_{ij,0}$complex power point in kVA used to inner approximate thermal constraint l on phase k of line (i, j) during disaster s.$R^{k_1k_2}_{ij}$resistance in ohms between phases k_1 and k_2 of line (i, j).$X^{k_1k_2}_{ij}$reactance in ohms between phases k_1 and k_2 of line (i, j).$\boldsymbol{Z}_{ij}3 \times 3$ impedance matrix in ohms of line (i, j), where element $Z_{ij}[k1, k2] = R^{k_1k_2}_{ij} + \mathbf{i}X^{k_1k_2}_{ij}$.$\bar{R}^{k_1k_2}_{ij}$resistance in ohms between phases k_1 and k_2 of line (i, j), rotated by $2\pi/3$.$\bar{X}^{k_1k_2}_{ij}$reactance in ohms between phases k_1 and k_2 of line (i, j), rotated by $2\pi/3$.$\bar{\boldsymbol{Z}}_{ij}3 \times 3$ impedance matrix in ohms of line (i, j), where element $\bar{Z}_{ij}[k1, k2] = \bar{R}^{k_1k_2}_{ij} + \mathbf{i}\bar{X}^{k_1k_2}_{ij}$ and $\bar{\boldsymbol{Z}}_{ij} = \boldsymbol{Z}_{ij}e^{\mathbf{i}2\pi/3}$.$\underline{R}^{k_1k_2}_{ij}$resistance in ohms between phases k_1 and k_2 of line (i, j), rotated by $-2\pi/3$.$\underline{X}^{k_1k_2}_{ij}$reactance in ohms between phases k_1 and k_2 of line (i, j), rotated by $-2\pi/3$.$\underline{\boldsymbol{Z}}_{ij}3 \times 3$ impedance matrix in ohms of line (i, j), where element $\underline{Z}_{ij}[k1, k2] = \underline{R}^{k_1k_2}_{ij} + \mathbf{i}\underline{X}^{k_1k_2}_{ij}$ and $\underline{\boldsymbol{Z}}_{ij} = \boldsymbol{Z}_{ij}e^{-\mathbf{i}2\pi/3}$.$\boldsymbol{V}^s_i$vector of complex voltage in kV on each of the three phases of node i during disaster s.$\boldsymbol{I}^s_{ij}$vector of complex current A on each of the three phases of branch ij during disaster s.$V^{s}_{i,k}$magnitude-squared of voltage in kV on phase k at node i during disaster s.V_{min}minimum magnitude-squared voltage in kV.V_{max}maximum magnitude-squared voltage in kV.Mvalid constant for disabling voltage constraints on nonexistent or open lines, where $M = 10^3(V_{max} - V_{min})$.$c_{ij}$cost in $ to build line (i, j); $0 if line already exists.ψ_{ij}cost in $ to harden line (i, j).$\alpha_l$cost in $ to build generator l.Variables$\boldsymbol{S}^{ds}_{i,k}$power in kVA delivered to phase k of load l during disaster s.y^s_ldetermines if the lth load is served or not during disaster s.$\boldsymbol{S}^{gs}_{i,k}$complex power in kVA produced by generator l on phase k during disaster s.$\boldsymbol{S}^{k,s}_{ij}$ $P^{k,s}_{ij} + \mathbf{i}Q^{k,s}_{ij}$: complex power in kVA flowing on each phase of line (i, j) from node i during disaster s.$\boldsymbol{S}^{k,s}_{ij}$ $P^{k,s}_{ij} + \mathbf{i}Q^{k,s}_{ij}$: complex power in kVA flowing on phase k of line (i, j) from node i during disaster s.e^s_{ij}determines if line (i, j) is used during disaster s.$e^s_{ij,0}$determines if flow exists on line (i, j) from j to i during disaster

$s.e^s_{ij,1}$determines if flow exists on line (i, j) from i to j during disaster s.b_{ij}determines if line (i, j) is built.h_{ij}determines if line (i, j) is hardened.$u_l$determines if generator l is constructed.h^s_{ij}determines if line (i, j) is hardened during disaster s.$\bar{b}^s_{ij}$determines if at least one edge between node i and node j is used during disaster s.

3. Formulation and algorithms

The resilient design problem presented here selects a set of network upgrades that will reduce load outaged during an extreme event. The objective selects the least expensive upgrade combination for a feeder, consisting of (i) adding switchable new lines to improve meshing, (ii) hardening lines, and (iii) adding generators that allow the feeder to meet resilience requirements. The generators interact with existing and new switches on the distribution system, allowing them to island and form microgrids. The resilience requirements are defined over a set of disaster scenarios. Each disaster scenario describes the power system after the event has disabled lines or other equipment. In this paper, the scenarios are obtained by sampling from a probability distribution of pole failure during ice and wind storms [25]. In general, these scenarios are created on a case-by-case basis depending on the extreme event of concern.

3.1. Metrics

The design criteria for resilience are (i) constraints for load served, and (ii) costs for the upgrades. The problem is formulated to upgrade an electrical distribution system to meet load constraints at a minimal cost. Load constraints consist of critical load served and noncritical load served. The load served criteria are defined in terms of the total power supplied to critical and noncritical loads in each damage scenario. In a typical design, a large majority (90–100%) of critical load is required to be met and 10–50% of noncritical load is required to be met. The noncritical load constraint encourages solutions that will help improve resiliency for regular customers while ensuring resilient power for critical loads.

Without loss of generality, new lines are constructed underground at a cost that is linear with respect to their length [26,27]. Although this study addresses only perfect hardening (underground lines for ice and wind storms), the problem formulation can be extended to address imperfect hardening options such as adding guy wires, adding composite crossarms, reducing vegetation, or increasing pole class. See [7] for how to model situations when new lines are not perfectly reliable. To ensure that the distribution system is operated radially, new lines always come with a switch.

This work assumes that hardening lines involves removal of the existing overhead line and replacement with an underground line. As with new lines, hardened lines are also perfectly reliable. It is also assumed that the cost of removal of the overhead line is small compared to that of the new underground line [28,29,2]. Thus, the cost is the same as adding a new underground line, with the exception that a switch is not added (therefore the additional cost of the switch does not apply). It is assumed that the existing feeder has sufficient switches to always operate in a radial configuration.

The cost of installing a generator consists of a fixed cost plus a variable cost that is linear in its power rating. The fixed cost includes balance-of-system costs, the generator fuel tank cost, the transfer switch cost, and the fixed portion of the generator cost [30].

3.2. Fragility model

This study is based on resilience to ice and wind storms [31]. The failure mode is ice accumulation on conductors and communications cables that increases the cross-sectional area such that wind pressure on the cables is sufficient to exceed the breaking strength of the pole. Underground lines are unaffected by this failure mechanism and are assumed to be perfectly reliable for the purposes of this study. The probability of pole failure is assumed to be uniform for each pole in the system, which corresponds to a uniform spatial distribution of wind speed and identical pole parameters. A more detailed analysis could account for differences between poles such as: pole geometry, pole spacing, wood density, wood tensile strength, conductor height, conductor thickness, conductor weight and observed wind speed [25]. The line failure probabilities are derived from the pole failure probabilities and are sampled to generate the set of disaster scenarios. Given a failure probability p_p for each pole, the line failure probability p_l is the likelihood of one of the poles supporting a line span failing

$$p_l = 1 - (1 - p_p)^2. \tag{1}$$

For each line span, a weighted coin is flipped to determine if the line fails in a particular disaster scenario. This is repeated for each disaster scenario.

3.3. Feasible operations

The set of scenarios S includes a set of disaster scenarios and the baseline scenario with no damage. Given a scenario $s \in S$, we define $Q(s)$ as a feasible operating point for a distribution network using Eq. (2). Here, the voltage drop across each line is enforced by Eq. (2a), whereas the power flow into each branch is enforced by Eq. (2b), where $(\cdot)^H$ denotes the Hermitian transpose. Line thermal limit constraints for active lines are enforced by Eq. (2c). When the line is not used, the flow is forced to 0 by $e^s_{ij} \in \{0, 1\}$. Voltage bounds are enforced using Eq. (2d). In Eq. (2e), $e^s_{ij,0} \in \{0, 1\}$ indicates that power on all phases flows in the forward direction on a line, whereas $e^s_{ij,1} \in \{0, 1\}$ indicates that power on all phases flows in the reverse direction. The equation requires that only one of these variables be active at a time, which forces all phases to flow in the same direction, an engineering constraint. Eq. (2f) states that the flow on a line is 0 when the line is not available (switch open or not built). Eq. (2g) limits the fractional flow imbalance between the phases to a value smaller than β_{ij}. Imbalance between phases cannot be extreme otherwise equipment may be damaged. Here, we use $\beta_{ij} = 0.15$ for transformers and $\beta_{ij} = 1.0$ otherwise. Eq. (2h) states that the flow on a line is 0 when the line is damaged and not hardened (recall that only existing lines are damageable here). Eq. (2i) requires all or none of the load at a bus to be served. Once again, this is an engineering limitation of most networks. Eq. (2j) limits the generator output by its capacity and caps the generation capacity that can be installed at each node. Eq. (2k) ensures flow balance at the nodes for all phases. The summation of $j \in \mathcal{N}$ collects edges oriented in the "from" direction connecting it's neighboring nodes. Eq. (2l) eliminates network cycles, forcing a tree or forest topology. Eq. (2m) ensures that a minimum fraction λ of critical load is served. Eq. (2n) ensures that a minimum fraction of noncritical load is served. Eqs. (2m) and (2n) are the resilience criteria that must be met and are similar to the $n - k - \epsilon$ criteria of [32]. Eq. (2o) states which variables are discrete.

Although the distribution networks studied here do not have parallel lines between the same node, the presence of such lines can greatly increase the number of constraints, which grows in a combinatorial fashion. When this issue arises, cycle constraints are enforced with a set of artificial cycle variables, as described in [7].

$$\boldsymbol{I}^s_{ij} = \begin{cases} \boldsymbol{Z}^{-1}_{ij}(\boldsymbol{V}^s_i - \boldsymbol{V}^s_j), & e^s_{ij} = 1 \\ 0, & e^s_{ij} = 0 \end{cases} \quad \forall\ ij \in \mathcal{E} \tag{2a}$$

$$\boldsymbol{S}^s_{ij} = \begin{cases} \mathrm{diag}(\boldsymbol{V}^s_i(\boldsymbol{I}^s_{ij})^H), & e^s_{ij} = 1 \\ 0, & e^s_{ij} = 0 \end{cases} \quad \forall\ ij \in \mathcal{E} \tag{2b}$$

$$|\boldsymbol{S}^{k,s,l}_{ij}|^2 \le (\bar{S}^k_{ij})^2 \quad \forall\ ij \in \mathcal{E},\ k \in \mathcal{P}_{ij} \tag{2c}$$

$$V_{\min} \le V^s_{i,k} \le V_{\max} \quad \forall\ i \in \mathcal{N},\ k \in \mathcal{P}_i \tag{2d}$$

$$e^s_{ij,0} + e^s_{ij,1} \leqslant e^s_{ij} \quad \forall\ ij \in \mathcal{E} \tag{2e}$$

$$e^s_{ij} = b^s_{ij} \quad \forall\ ij \notin \mathcal{D}_s \tag{2f}$$

$$\frac{\sum_{k\in\mathcal{P}_{ij}} \boldsymbol{S}^{k,s}_{ij}}{\frac{|\mathcal{P}_{ij}|}{(1-\beta_{ij})}} \leqslant \boldsymbol{S}^{k',s}_{ij} \leqslant \frac{\sum_{k\in\mathcal{P}_{ij}} \boldsymbol{S}^{k,s}_{ij}}{\frac{|\mathcal{P}_{ij}|}{(1+\beta_{ij})}} \quad \forall\ ij \in \mathcal{E},\ k' \in \mathcal{P}_{ij} \tag{2g}$$

$$e^s_{ij} = h^s_{ij}\ \forall\ ij \in \mathcal{D}_s \tag{2h}$$

$$\boldsymbol{S}^{ds}_{i,k} = \sum_{l\in\mathcal{L}_i} \bar{\boldsymbol{S}}^d_{l,k} y^s_l \quad \forall\ i \in \mathcal{N},\ k \in \mathcal{P}_i \tag{2i}$$

$$\boldsymbol{S}^{gs}_{i,k} \leqslant \sum_{l\in\mathcal{G}_i} \bar{\boldsymbol{S}}^g_{l,k} u_l \quad \forall\ i \in \mathcal{N},\ k \in \mathcal{P}_i \tag{2j}$$

$$\boldsymbol{S}^{gs}_{i,k} - \boldsymbol{S}^{ds}_{i,k} - \sum_{j\in\mathcal{N}} \boldsymbol{S}^{k,s}_{ij} = 0 \quad \forall\ i \in \mathcal{N},\ k \in \mathcal{P}_i \tag{2k}$$

$$\sum_{ij\in\mathcal{E}(C)} e^s_{ij} \leqslant |\mathcal{E}(C)| - 1 \quad \forall\ C \in C \tag{2l}$$

$$\sum_{i\in\mathcal{N}(\mathcal{K}),k\in\mathcal{P}_i} \boldsymbol{S}^{ds}_{i,k} \geqslant \lambda \sum_{l\in\mathcal{K},k\in\mathcal{P}_l} \bar{\boldsymbol{S}}^d_{l,k} \tag{2m}$$

$$\sum_{i\in\mathcal{N},k\in\mathcal{P}_i} \boldsymbol{S}^{ds}_{i,k} \geqslant \gamma \sum_{l\in\mathcal{L},k\in\mathcal{P}_l} \bar{\boldsymbol{S}}^d_{l,k} \tag{2n}$$

$$b^s_{ij},\ h^s_{ij},\ w^s_{ij},\ e^s_{ij},\ y^s_l,\ u_l \in \{0,\ 1\} \tag{2o}$$

3.4. Tractable approximation of feasibility

In the formulation of $Q(s)$, Eqs. (2a, 2b), and (2c) are the most difficult to handle from a computational perspective. Here, Eqs. (2a) and (2b) are not convex. Although Eq. (2c) is a convex quadratic constraint, such constraints can be numerically difficult for modern mixed-integer solvers to handle. To address this computational challenge, we approximate Eqs. (2a) and (2b) with Eq. (3) from [14].

$$-M(1-e^s_{ij}) \leq 10^3(V^s_{j,a} - V^s_{i,a}) + 2(R^{aa}_{ij} P^{a,s}_{ij} + X^{aa}_{ij} Q^{a,s}_{ij} + \bar{R}^{ab}_{ij} P^{b,s}_{ij} + \bar{X}^{ab}_{ij} P^{b,s}_{ij} + \underline{R}^{ac}_{ij} P^{c,s}_{ij} + \underline{X}^{ac}_{ij} Q^{c,s}_{ij}) \leq M(1-e^s_{ij}) \quad \forall\ i \in \mathcal{N} \tag{3a}$$

$$-M(1-e^s_{ij}) \leq 10^3(V^s_{j,b} - V^s_{i,b}) + 2(\underline{R}^{ba}_{ij} P^{a,s}_{ij} + \underline{X}^{ba}_{ij} Q^{a,s}_{ij} + R^{bb}_{ij} P^{b,s}_{ij} + X^{bb}_{ij} P^{b,s}_{ij} + \bar{R}^{bc}_{ij} P^{c,s}_{ij} + \bar{X}^{bc}_{ij} Q^{c,s}_{ij}) \leq M(1-e^s_{ij}) \quad \forall\ i \in \mathcal{N} \tag{3b}$$

$$-M(1-e^s_{ij}) \leq 10^3(V^s_{j,c} - V^s_{i,c}) + 2(\bar{R}^{ca}_{ij} P^{a,s}_{ij} + \bar{X}^{ca}_{ij} Q^{a,s}_{ij} + \underline{R}^{cb}_{ij} P^{b,s}_{ij} + \underline{X}^{cb}_{ij} P^{b,s}_{ij} + R^{cc}_{ij} P^{c,s}_{ij} + X^{cc}_{ij} Q^{c,s}_{ij}) \leq M(1-e^s_{ij}) \quad \forall\ i \in \mathcal{N} \tag{3c}$$

Here, Eqs. (3a) to (3c) define the linearized voltage drops across lines where the variables $V^s_{i,k}$ model the voltage magnitude-squared on phase k of node i under scenario s. We then approximate Eq. (2c) with Eq. (4).

$$-e^s_{ij,0} P^{k,s,l}_{ij,0} \leqslant P^{k,s}_{ij} \leqslant e^s_{ij,1} P^{k,s,l}_{ij,0} \quad \forall\ ij \in \mathcal{E},\ k \in \mathcal{P}_{ij},\ l \in \{3,\ 7\} \tag{4a}$$

$$-e^s_{ij,0} Q^{k,s,l}_{ij,0} \leqslant Q^{k,s}_{ij} \leqslant e^s_{ij,1} Q^{k,s,l}_{ij,0} \quad \forall\ ij \in \mathcal{E},\ k \in \mathcal{P}_{ij},\ l \in \{1,\ 5\} \tag{4b}$$

$$P^{k,s,l}_{ij,0} P^{k,s}_{ij} + Q^{k,s,l}_{ij,0} Q^{k,s}_{ij} \leqslant ((P^{k,s,l}_{ij,0})^2 + (Q^{k,s,l}_{ij,0})^2) \quad \forall\ ij \in \mathcal{E},\ k \in \mathcal{P}_{ij},\ l \in \{2,\ 4,\ 6,\ 8\} \tag{4c}$$

Here, Eqs. (4a) to (4c) model an inner approximation of the capacity constraint on power flow for each phase of a line based on a polygon enclosed by eight lines. This approximation is illustrated in Fig. 1. In the figure, the outer circle is the actual line thermal limit. The inner circle is the thermal limit scaled such that an octagon whose edges are tangent to the inner circle and whose vertices intersect the outer circle exists. This octagon describes a feasible region for $Q(s)$, and the bold points mark the $(P^{k,s,l}_{ij,0},\ Q^{k,s,l}_{ij,0})$ points in Eqs. (4a) to (4c). These points indicate where on the circle for the thermal limit the constraint is linearized to approximate it as a polygon. The full approximation of $Q(s)$, denoted by $Q'(s)$, is then defined by Eqs. (2d)–(3), and (4).

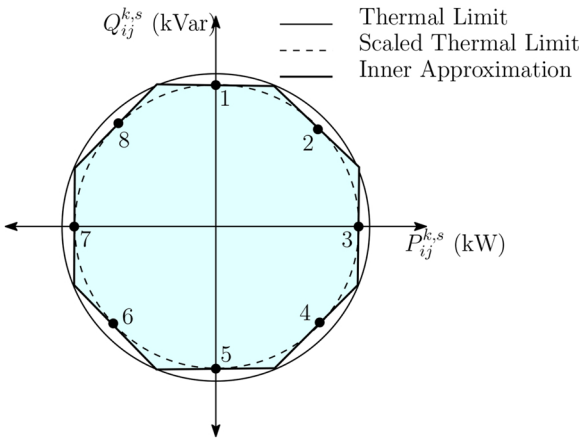

Fig. 1. Inner approximation of line thermal limit constraints.

3.5. Optimal design

The resilient design optimization problem is the network upgrade that has minimum cost and satisfies $Q'(s)$, i.e.,

$$P(S) = \min\ \textstyle\sum_{ij\in\mathcal{E}} (c_{ij} b_{ij} + \psi_{ij} h_{ij}) + \sum_{l\in\mathcal{G}} \alpha_l u_l \tag{5a}$$

s. t.

$$b^s_{ij} \leqslant b_{ij} \quad \forall\ ij \in \mathcal{E},\ s \in \mathcal{S} \tag{5b}$$

$$h^s_{ij} = h_{ij} \quad \forall\ ij \in \mathcal{E},\ s \in \mathcal{S} \tag{5c}$$

$$b_{ij},\ h_{ij},\ u_l \in \{0,\ 1\} \quad \forall\ ij \in \mathcal{E},\ l \in \mathcal{G} \tag{5d}$$

$$(b^s_{ij},\ h^s_{ij},\ u_l) \in Q'(s) \quad \forall\ s \in \mathcal{S} \tag{5e}$$

Eq. (5a) minimizes the cost of constructing new lines, hardening existing lines, and installing generators. The generators have fixed sizes, and the cost of each generator is split into a fixed installation cost and a cost based on its capacity. Eqs. (5b) through (5e) link the first-stage and second-stage variables ($Q'(s)$). The inequality in Eq. (5b) allows new lines to be switched. Eq. (5e) states that the vector of continuous and discrete variables (b_{ij}, h_{ij}, u_l) is a feasible network for scenario s. Note that $b^s_{ij} = 1$ for all existing lines in the network. Similarly, $h^s_{ij} = 0$ for all candidate new lines.

3.6. Algorithm

The problem is solved using scenario-based decomposition (SBD) [7]. SBD solves the mixed-integer network upgrade problem for the base case and a single scenario and then evaluates the designed network on the remaining scenarios to verify whether it is feasible. If the designed network is not feasible on any one of the remaining disaster scenarios, the infeasible scenario with the highest amount of load shedding is added to the upgrade problem and the process is repeated until feasibility is reached. SBD exploits the property of the problem that once the network is designed, the solutions for each scenario are independent of each other. Formally, the algorithm is described in Algorithm 1. Here, line 2 solves the optimization problem defined by Eqs. (5a) to (5e) on the set S'. Line 3 then determines the maximum violation of the resilience metrics for the design solution given by σ^*. Line 3 calculates the violation by solving the following optimization problem:

$$F(s,\ \sigma = b,\ h,\ u) = \min\ \ \nu + \mu \tag{6a}$$

s. t.

$$(2d) - (2l); (2n); (2o); 3; 4 \tag{6b}$$

$$\nu + \sum_{i\in\mathcal{N}(\mathcal{K}),k\in\mathcal{P}_i} \boldsymbol{S}^{\mathrm{ds}}_{i,k} \geqslant \lambda \sum_{l\in\mathcal{K},k\in\mathcal{P}_l} \bar{\boldsymbol{S}}^{d}_{l,k} \tag{6c}$$

$$\mu + \sum_{i\in\mathcal{N},k\in\mathcal{P}_i} \boldsymbol{S}^{\mathrm{ds}}_{i,k} \geqslant \gamma \sum_{l\in\mathcal{L},k\in\mathcal{P}_l} \bar{\boldsymbol{S}}^{d}_{l,k} \tag{6d}$$

If all resilience criteria are satisfied, then σ^* is optimal and this solution is returned (line 4). Otherwise, the scenario with the worst resilience violation is added to $\mathcal{S}'$ and the process repeats (line 6). Line 7 returns the optimal solution and certificate that validates the feasibility of σ^*. Here, OpenDSS is used for validation. Interestingly, as shown in the results, this approach scales well to very large systems.

Algorithm 1. Scenario-Based Decomposition

Input: A set of disasters $\mathcal{S}$ and let $\mathcal{S}' = \{\mathcal{S}_0\}$;

1 **while** $\mathcal{S} \setminus \mathcal{S}' \neq \emptyset$ **do**
2 $\sigma^* \leftarrow$ Solve $\mathcal{P}(\mathcal{S}')$;
3 **if** $\max_{s\in\mathcal{S}\setminus\mathcal{S}'} \mathcal{F}(s,\sigma^*) \leq \langle 0,0\rangle$ **then**
4 **return** σ^*;
5 **else**
6 $\mathcal{S}' \leftarrow \mathcal{S}' \cup \arg\max_{s\in\mathcal{S}\setminus\mathcal{S}'} \mathcal{F}(s,\sigma^*)$;
7 **return** $\langle \sigma^*, \mathrm{Validate}(\sigma^*)\rangle$

4. Numerical experiments

The case studies in this paper are based on two feeders from a distribution system in the northeast United States. Each feeder is served by a different substation, and the feeders are meshed so that they can be backfed from one another.

4.1. Implementation

Results are based on a C++ implementation using CPLEX 12.6.2 as the mixed-integer linear programming solver. All studies were run on a server with 64 GB of memory and two 2.6 GHz Intel(r) Xeon(r) E5-2660 v3 processors, where 32 threads were used.

4.2. Case study systems

Three case studies are considered. The first two consider the feeders operating individually, whereas the combined case study focuses on the advantages of meshing systems as networked microgrids. Table 1 summarizes the salient characteristics of the two feeders, which are illustrated in Fig. 2. The utility systems are unmodified with the exception that line charging capacitances are not included.

Case Study 1 is the smaller feeder. It has two three-phase trunks connected to the substation by an underground line and feeds a mix of mostly overhead and underground single-phase laterals with occasional three-phase laterals. It serves a relatively small number of critical loads. Case Study 2 is the larger feeder, with critical loads distributed throughout. It has a long looping overhead three-phase trunk connected to a second main trunk and also serves a mix of mostly overhead and underground single-phase laterals.

Table 2 summarizes the upgrade options for the case studies. Generators can be installed only at critical loads. In Fig. 2, line segments that can be hardened via undergrounding are green. These segments can form an alternate path to supply critical loads. Candidate new lines are indicated with violet dashed lines. Only a small number are present,

Table 1
Case study system properties

Parameter	Case Study 1	Case Study 2
Number of buses	271	945
Number of lines	281	940
Total number of loads	125	333
Total load power	5.50 MW	7.64 MW
Number of critical loads	3	6
Total critical load power	359 kW	972 kW
Approximate span east-west	1.5 km	2.1 km
Approximate span north-south	1.2 km	2.3 km

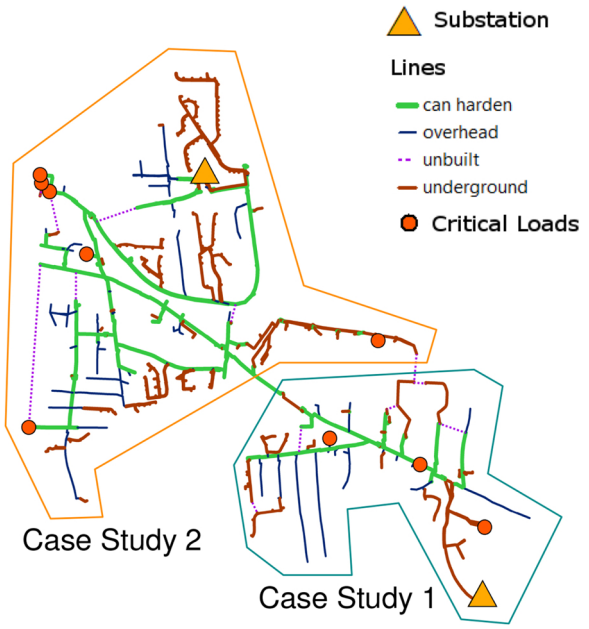

Fig. 2. Case Study 1 and Case Study 2 feeders.

and they are placed only if they are well suited to provide alternate paths of power between a substation and critical loads or between critical loads.

The criteria and costs used in the case studies are summarized in Table 3. The critical load–served requirements are 98% for Case Study 1 and 90% for the other cases. The amount of noncritical load that must be served varies between 10 and 50%. Depending on the amount of noncritical load, the optimizer will select a solution that can also provide power to noncritical loads (low amount of noncritical load required to be served) or a solution that adds additional hardening specifically to provide power to a sufficient amount of noncritical loads (high amount of noncritical load required to be served).

Each potential generator location has the choice of 10 sizes between 100 kW and 1 MW in 100 kW increments. As described earlier, the cost of adding generators consists of a fixed portion and a capacity-based portion that is linear in the power rating. We perform a sensitivity analysis on the capacity-based portion of the cost. The cost of new lines and upgrading lines remains constant across all design cases studied. Each of 50 damage scenarios is constructed by damaging lines with a 20% probability. The number of damage scenarios and probability are

Table 2
Problem setup properties

Parameter	Case Study 1	Case Study 2	Case Study 1 + 2
Generators	3	6	9
Candidate lines	6	6	12
Upgradeable lines	148	462	610

Table 3
Constant parameters for all case studies

Parameter	Value
Phase variation	15%
Critical load served	90%, 98%
Noncritical load served	10%, 20%,... 50%
Microgrid sizing increment[a]	100 kW
Microgrid fixed cost	$25k
Maximum microgrid size	1 MW
Microgrid variable cost[b]	$100/kW, $200/kW,... $500/kW
Line hardening cost	$1M/mile
New (Underground) cost	$1M/mile + $25k
Damage probability per line	20%
Number of damage scenarios	50

[a] Power is given per phase.
[b] Costs are given in terms of dollars per average power per phase.

selected to obtain a sufficient number of outaged line segments across all scenarios for the optimizer to converge on a solution.

For Case Study 1 and Case Study 2, we perform a sensitivity analysis on the noncritical load served and generator capacity cost parameters. For Case Study 1, 5 values are used for each parameter, giving 25 design cases. For Case Study 2, 9 values are used for each parameter, giving 81 cases. For the combined Case Study 1 + 2 feeder, a single design case is discussed.

5. Results

The results demonstrate three of the key contributions of this paper: the verification of the scalability of the resilient design algorithm, the validity of the design solutions based on the approximation used in this paper, and the value of networking microgrids in conjunction with other resiliency options, such as hardening. Results from the sensitivity analysis for Case Study 1 are shown in Fig. 3. The center contour plot depicts the difference between the amount of microgrid generation installed in tens of kW and the total number of hardened/new lines. As the amount of noncritical load required to be served increases, the solution starts to include hardening of the feeder trunk. As the cost of installing a generator increases, the solution starts to include hardening of paths to critical loads instead of installing generators. The overall trend from the bottom left to the top right increasingly favors lines over generators. The critical load closest to the substation never receives a generator because it is connected via a three-phase underground line to the substation and is never damaged under the studied threat scenario. In case (b) at the top right of the figure, one critical load receives neither a generator nor a hardened path. The result is reasonable given that it is a small amount of the total critical load so the 98% critical load–served criteria are not violated.

Results from the sensitivity analysis for Case Study 2 are displayed in Fig. 4. The number of new and hardened lines increases as the noncritical load served increases and the generator variable cost increases. However, total generator power rating becomes more sensitive with respect to generator variable cost as the amount of noncritical load served increases. In case (a), inexpensive microgrid generation supplies noncritical loads instead of new or hardened lines, as in case (b). In all cases, the critical loads in the top left of the network figure are connected via hardened lines as a collection of networked microgrids. In case (b), the lines are built to supply noncritical loads and the critical load at the bottom right of the diagram. Results for the Case Study 1 + 2 meshed system are illustrated in Fig. 5 with a microgrid variable cost of $500/kW and 33% noncritical load served. This solution has a smaller set of networked microgrids shown at the top left of the figure. Also of interest is that a new line is constructed to increase meshing of the two feeders, allowing a critical load in Case Study 2 to draw power from the Case Study 1 substation with only a small amount of hardening of the Case Study 1 feeder trunk.

The three combinations of feeders are compared in Table 4 with parameters of $500/kW generator cost and 33% noncritical load served. For all combinations, 90% of critical load must be served. This table supports one of the key contributions of this manuscript: *a demonstration on utility data that networked microgrids can bring strong resilience benefits*. The cost of making each microgrid resilient independently is roughly $2M. However, meshing the feeders and allowing them to support each other results in a resilient system costing roughly one-third of the independent solutions.

In terms of computation time, the design problem took between 3 and 6 minutes for Case Study 1 and between 1 and 3 hours for Case Study 2 and Case Study 1 + 2. Simulation results from OpenDSS verified that the designed solutions do not result in voltage violations, with the observed voltages ranging from 0.993 to 1.031 per unit across all case study systems and damage scenarios.

6. Conclusions

We developed and applied a method for improving distribution resilience on large-scale distribution systems. Our study supports claims

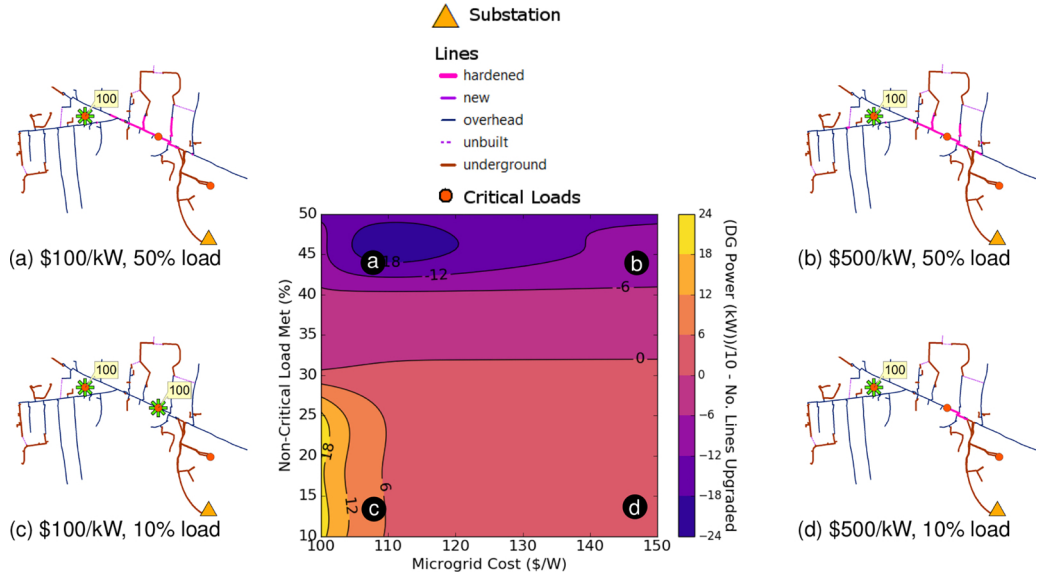

Fig. 3. Case Study 1 microgrid construction metric and solutions.

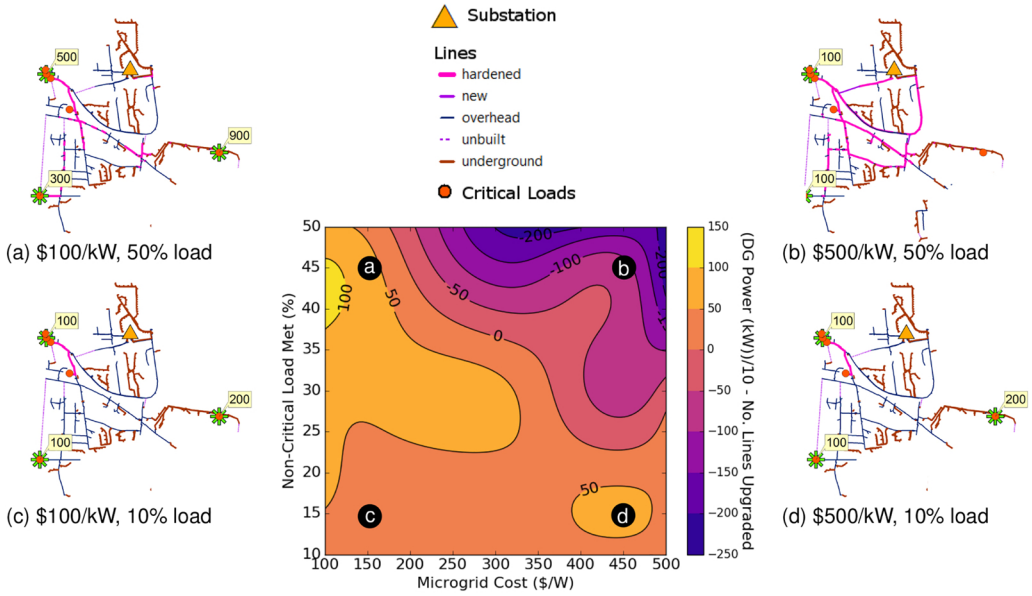

Fig. 4. Case Study 2 microgrid construction metric and solutions.

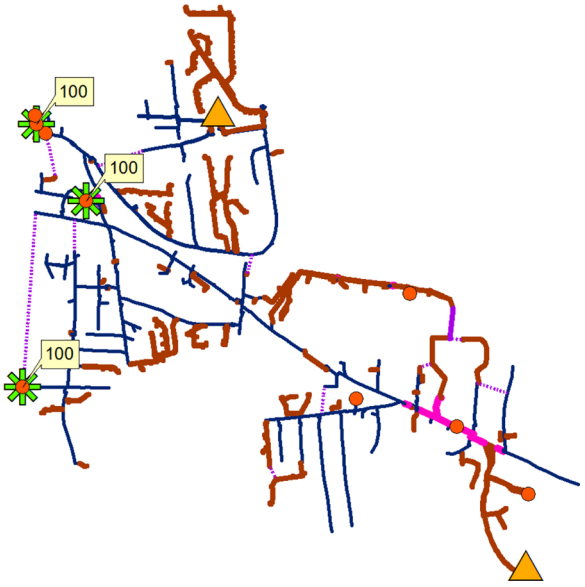

Fig. 5. Case Study 1 + Case Study 2 solution.

Table 4
Comparison of costs for feeders

Item	Case Study 1	Case Study 2	Case Study 1 + 2
Cost	$224k	$1.72M	$720k
New lines	0	2	1
Hardened lines	12	82	24
Number of generators	1	1	3
Generator power (kW)	100	100	300

for the key benefits of the method, including scalability to large-scale systems, ability to handle unbalanced AC power flow physics, and resilient design that includes hardening, redundancy, and networked microgrids. Interestingly, our results support the claim that there are situations where networked microgrids are the most cost-effective option for improving the resilience of distribution feeders. More specifically, networked microgrids provide value when there are clusters of critical loads that are distant from a substation and the cost of hardening lines is higher than the cost of installing generators. As the cost of hardening decreases, the benefit of using networked microgrids also decreases. Our results also indicate that the cost of upgrading the resilience of two or more feeders together can be significantly less than upgrading them individually. To evaluate the cost of upgrading feeders across a large distribution system provider would require running the optimization across the system. However it is expected that the averaged hardening cost will be lower than the two feeders considered here, as mutual support between feeders will reduce the upgrade cost and not all feeders will include critical loads. Although this work made significant strides in developing the methods and techniques necessary to create tools that support resilience planning for distribution systems, there remain a number of future directions for this work. First, it will be important to develop global optimization methods for recovering feasible solutions in situations where the approximations used here do not result in feasible solutions. Second, recent advances in convex relaxations to the unbalanced AC power flow physics would be interesting to include in the modeling, in particular when meshed networks are allowed [14]. Finally, it will be interesting to further improve the scaling to cover systems with potentially tens of thousands of nodes and edges.

Funding

The work was funded by the DOE-OE Smart Grid R&D Program in the Office of Electricity in the US Department of Energy. It was carried out under the auspices of the NNSA of the U.S. DOE at LANL under Contract No. DE-AC52-06NA25396.

References

[1] Y. Wang, C. Chen, J. Wang, R. Baldick, Research on resilience of power systems under natural disasters; a review, IEEE Trans. Power Syst. 31 (2) (2016) 1604–1613.
[2] T. Gonen, Electric Power Distribution Engineering, CRC press, 2016.
[3] S. Ma, B. Chen, Z. Wang, Resilience enhancement strategy for distribution systems under extreme weather events, IEEE Transactions on Smart Grid PP (99) (2016) 1-1.
[4] D.T. Ton, W.P. Wang, A more resilient grid: The US department of energy joins with stakeholders in an R&D plan, IEEE Power Energy Mag. 13 (3) (2015) 26–34.
[5] M. Shahidehpour, x. liu, Z. Li, Y. Cao, Microgrids for enhancing the power grid resilience in extreme conditions, IEEE Transactions on Smart Grid PP (99) (2016) 1-1.
[6] Z. Li, M. Shahidehpour, F. Aminifar, A. Alabdulwahab, Y. Al-Turki, Networked microgrids for enhancing the power system resilience, Proc. IEEE 105 (7) (2017) 1289–1310.
[7] E. Yamangil, R. Bent, S. Backhaus, Resilient upgrade of electrical distribution grids,

in: Proceedings of the Association for the Advancement of Artificial Intelligence (2015) 1233–1240.
[8] H. Gao, Y. Chen, Y. Xu, C. C. Liu, Resilience-oriented critical load restoration using microgrids in distribution systems, IEEE Transactions on Smart Grid PP (99) (2016) 1-1.
[9] G. Byeon, P. Van Hentenryck, R. Bent, H. Nagarajan, Communication-constrained expansion planning for resilient distribution systems, arXiv preprint arXiv:1801.03520.
[10] L.G. Valiant, The complexity of enumeration and reliability problems, SIAM J. Comput. 8 (3) (1979) 410–421.
[11] R.A. Jabr, Polyhedral formulations and loop elimination constraints for distribution network expansion planning, IEEE Trans. Power Syst. 28 (2) (2013) 1888–1897.
[12] H. Nagarajan, S. Rathinam, S. Darbha, On maximizing algebraic connectivity of networks for various engineering applications, in: European Control Conference, IEEE (2015) 1626–1632.
[13] E. Dall'Anese, H. Zhu, G.B. Giannakis, Distributed optimal power flow for smart microgrids, IEEE Trans. Smart Grid 4 (3) (2013) 1464–1475.
[14] L. Gan, S.H. Low, Convex relaxations and linear approximation for optimal power flow in multiphase radial networks, in: Power Systems Computation Conference (PSCC), 2014, IEEE, 2014, pp. 1–9.
[15] M. D. Sankur, R. Dobbe, E. Stewart, D. S. Callaway, D. B. Arnold, A linearized power flow model for optimization in unbalanced distribution systems, arXiv preprint arXiv:1606.04492.
[16] K. Christakou, D.-C. Tomozei, J.-Y. Le Boudec, M. Paolone, AC OPF in radial distribution networks - Part I: On the limits of the branch flow convexification and the alternating direction method of multipliers, Electric Power Syst. Res. 143 (Supplement C) (2017) 438–450.
[17] K. Christakou, D.-C. Tomozei, J.-Y. Le Boudec, M. Paolone, AC OPF in radial distribution networks - Part II: An augmented Lagrangian-based OPF algorithm, distributable via primal decomposition, Electric Power Syst. Res. 150 (Supplement C) (2017) 24–35.
[18] R.C. Dugan, T.E. McDermott, An open source platform for collaborating on smart grid research, in: Power and Energy Society General Meeting, IEEE (2011) 1–7.
[19] C. Yuan, M.S. Illindala, A.S. Khalsa, Modified viterbi algorithm based distribution system restoration strategy for grid resiliency, IEEE Trans. Power Del. 32 (1) (2017) 310–319.
[20] T. Ding, Y. Lin, G. Li, Z. Bie, A new model for resilient distribution systems by microgrids formation, IEEE Transactions on Power Systems PP (99) (2017) 1-1.
[21] W. Yuan, J. Wang, F. Qiu, C. Chen, C. Kang, B. Zeng, Robust optimization-based resilient distribution network planning against natural disasters, IEEE Transactions on Smart Grid PP (99) (2016) 1-10.
[22] C. Chen, J. Wang, F. Qiu, D. Zhao, Resilient distribution system by microgrids formation after natural disasters, IEEE Trans. Smart Grid 7 (2) (2016) 958–966.
[23] L. Che, M. Shahidehpour, A. Alabdulwahab, Y. Al-Turki, Hierarchical coordination of a community microgrid with ac and dc microgrids, IEEE Trans. Smart Grid 6 (6) (2015) 3042–3051.
[24] L. Ren, Y. Qin, Y. Li, P. Zhang, B. Wang, P.B. Luh, S. Han, T. Orekan, T. Gong, Enabling resilient distributed power sharing in networked microgrids through software defined networking, Appl. Energy 210 (2018) 1251–1265.
[25] Y. Sa, Reliability analysis of electric distribution lines, Master's thesis, McGill University, Montreal, Canada (Jul. 2002). URL http://digitool.library.mcgill.ca/R/?func=dbin-jump-full&object_id=29546&local_base=GEN01-MCG02.
[26] S. S. J. Kurtz, G. Saur, C. Ainscough, Utilization of underground and overhead power lines in the city of new york, Tech. Rep. NREL/TP-5400-60732, Office of Long-Term Planning and Sustainability, Office of the Mayor, City of New York (Dec. 2013).
[27] C. M. Theodore V. Morrison, M. C. Christie, Placement of utility distribution lines underground, Tech. Rep. House Document No. 30, Governor and General Assembly of Virginia (Jan. 2005).
[28] J. Troy, Feasibility study for undergrounding electric distribution lines in Massachusetts, Tech. rep., Massachusetts Department of Energy Resources (Dec. 2014). URL https://www.mass.gov/files/documents/2016/08/od/under-grounding-distribution-lines.pdf.
[29] R. L. Ehrlich, M. S. Steele, R. L. Flanagan, N. J. Pederson, Cost benefits for overhead/underground utilities, no. SP208B4C, 2003. URL http://www.roads.maryland.gov/opr_research/md-03-sp208b4c-cost-benefits-for-overhead-vs-underground-utility-study_report.pdf.
[30] S. S. J. Kurtz, G. Saur, C. Ainscough, Backup power cost of ownership analysis and incumbent technology comparison, Tech. Rep. NREL/TP-5400-60732, National Renewable Energy Lab (Sep. 2014).
[31] Y. Sa, Reliability analysis of electric distribution lines, Master's thesis, McGill University, 2002.
[32] W. Yuan, L. Zhao, B. Zeng, Optimal power grid protection through a defender-attacker-defender model, Reliabil. Eng. Syst. Safety 121 (2014) 83–89.